

# CO<sub>2</sub> WHOLE AREA IRRADIATIVE PROCESSING AND PATTERNING OF NYLON 6,6 AND THE EFFECTS THEREOF ON OSTEOBLAST CELL RESPONSE IN RELATION TO WETTABILITY.

Paper (Paper Number)

David G. Waugh<sup>1</sup> and Jonathan Lawrence<sup>2</sup>

<sup>1</sup> Wolfson School of Mechanical and Manufacturing Engineering, Loughborough University, Loughborough, Leicestershire, LE11 3TU, UK.

<sup>2</sup>The Automotive Company, Address, City, State, Postal Code, Country

## Abstract

CO<sub>2</sub> laser processing of nylon 6,6 can modify its wettability and biomimetic characteristics. This paper discusses comparatively the use of a CO<sub>2</sub> laser for surface patterning and whole area processing, detailing the effects on the wettability and osteoblast cell response. White light interferometry found that the largest increase in surface roughness, with an Sa of 4 μm was obtained with the large area processed sample using an irradiance of 510 Wcm<sup>-2</sup>. The surface oxygen content was increased by up to 5 %at for all laser irradiated samples. A sessile drop device determined that the laser patterned samples gave rise to an increase in contact angle, whereas a decrease in contact angle was observed for the large area patterned samples in comparison to the as-received nylon 6,6. The increase in contact angle is explained by the likely existence of a mixed-state wetting regime. The bioactive nature of the samples were analysed by seeding osteoblast cells onto the nylon 6,6 samples for 4 days. It was found that most laser surface treated samples gave rise to a more biomimetic surface. Some samples gave a less enhanced biomimetic which can be attributed to an increase in surface toxicity. Also, generic wettability characteristics have been forged which can predict the biomimetic nature of laser surface treated nylon 6,6.

## Introduction

With biotechnology having the potential to improve quality of life it can be seen that there is ever increasing interest in this field. There usually has to be a compromise between bulk and surfaces properties. Where, in most cases the bulk properties are seen more in favour over those surface properties required [1]. As a result of this, the surface properties are usually not sufficient for the bioactivity required giving rise to clinical failure of the implant [1-4]. Therefore, it is

crucial to change the surface properties of the polymer allowing it to become more biomimetic.

Owed to the material properties nylon 6,6 possesses it can be seen that this polymer has been used for such biological applications as sutures, tracheal tubes and gastrointestinal segments [5]. What is more, by modifying the surface of polymeric materials it may be possible to identify other biological applications.

The role of wettability in biomaterials science has been one of the most interesting subject areas in biomaterials surface science for a number of years and has allowed many to endeavour to determine the complex links between surface wetting and bioactivity. A number of theories have been put forward, all having a common fundamental factor in which the surface energy/wetting is related somewhat to the biological response [6].

It has been seen through prior research that other methods [7-9] offer the ability to vary the physiochemical properties of the polymer surface without changing the bulk properties. These various techniques have the ability to improve cell growth and adhesion on polymeric biomaterials; however controlled, precise modification is lacking from the methods, are not usually cost-effective and in the most part, require a number of post-processes. Laser-induced surface treatment offers the ability to vary the physiochemical surface properties in a non-contact setup with considerably more control and accuracy.

From previous work [10] it has been shown that CO<sub>2</sub> laser patterning holds the ability to promote biomimetic characteristics of nylon 6,6 for osteoblast cells. Following on, this paper details a comparative study between CO<sub>2</sub> laser patterning and whole area irradiative processing of nylon 6,6 and the effects thereof on wettability characteristics. In addition, osteoblast cell response of each sample is considered

in terms of cell adhesion, proliferation and morphology.

## Experimental Technique

### Laser Processing

The nylon 6,6 was sourced in 100×100 mm<sup>2</sup> sheets with a thickness of 5 mm (Goodfellow Cambridge, Ltd). To obtain a conveniently sized sample for experimentation the as-received nylon sheet was cut into 30 mm diameter discs using a 1 kW continuous wave (cw) CO<sub>2</sub> laser (Everlase S48; Coherent, Ltd).

### Laser-Induced Patterning

In order to generate the required marking pattern with the 10.6 μm Synrad cw 10W CO<sub>2</sub> laser system Synrad Winmark software version 2.1.0, build 3468 was used. The nylon 6,6 samples were placed into the laser system onto a stage and held in place using a bracket. The surface of the sample was set to be 250 mm away from the output facet of the laser system to obtain focus and the system utilized a galvanometer scanner to scan the 95 μm spot size beam. It should be noted that the target material and laser system was held in a laser safety cabinet in which the ambient gas was air and an extraction system was used to remove any fumes produced during laser processing.

20 samples were patterned altogether to produce 4 identical 6-well plates. These were named plates 1, 2, 3 and 4. There were four patterns induced onto the surfaces of the nylon 6,6 samples which were trenches with 50 μm spacing (T50), hatch with 50 μm spacing (H50), trenches with 100 μm spacing (T100) and hatch with 100 μm spacing (H100). In addition, an as-received control sample was used (AR). For each of the irradiated patterns the laser power was set to 70% (7 W) operating at 600 mm<sup>-1</sup>.

### Whole Area Irradiative Processing

A cw 100 W CO<sub>2</sub> laser (DLC; Spectron, Ltd) was used to scan a 5mm diameter beam across the target sample with one pass in order to irradiate the test area with an irradiance of 510 Wcm<sup>2</sup>. By using a galvanometer, scanning speeds of 150, 100, 75, 50, 25 and 20 mm<sup>-1</sup> were employed to irradiate 6 samples with effective fluences of 16.84 (samples WA17), 25.51 (sample WA26), 34.18 (sample WA34), 51.02 (sample WA51), 102.04 (sample WA102) and 127.55 Jcm<sup>-2</sup> (sample WA128), respectively.

Also, similarly to the laser patterned samples 24 samples were irradiated as stated above to produce 4

identical 6-well plates; these being labelled as 1, 2, 3 and 4.

### Topography, Wettability Characteristics and Surface Chemistry Analysis

With regards to Plate 1, the surface profiles were determined using a white light interferometer (WLI) (NewView 500; Zygo, Ltd) with MetroPro and TalyMap Gold Software. The Zygo WLI was setup using a ×10 Mirau lens with a zoom of ×0.5 and working distance of 7.6 mm. This system also allowed Sa and Ra roughness parameters to be determined.

In accordance with Rance [11], the samples were ultrasonically cleaned in isopropanol (Fisher Scientific Ltd., UK) for 3 minutes at room temperature. A sessile drop device (OCA20; Dataphysics Instruments, GmbH) was then used with relevant software (SCA20; Dataphysics Instruments, GmbH) to allow the recent advancing for triply distilled water and diodomethane to be determined. The advancing contact angles for the two liquids were used by the software to draw an Owens, Wendt, Rabel and Kaebel (OWRK) plot to determine the surface energy of the samples. For the two reference liquids the SCA20 software used the Ström et al. technique to calculate the surface energy. It should be noted here that ten contact angles, using two droplets, in each instance was recorded to achieve a mean contact angle for each liquid and surface.

All samples were analysed using x-ray photoelectron spectroscopy (XPS) analysis. This allowed any surface modifications in terms of surface oxygen content due to the laser irradiation to be revealed.

### *In Vitro* Experimentation

Prior to any biological testing being carried out the samples were autoclaved (D-Series Bench-Top Autoclave; Systec, GmbH). For all biological work undertaken a biological safety cabinet (BSC) (Microflow Class II ABS Cabinet; BioQuell UK, Ltd) was used to create a clean, sterile environment.

Normal human osteoblast cells (Clonetics CC-2538; Lonza, Inc.) were initially cultured in a T75 (75ml) flask by suspending the cells in 19 ml culture medium comprising of 90% eagle minimum essential medium (Sigma-Aldrich, UK) and 10% foetal bovine serum (FBS) (Sigma-Aldrich, UK). After 24 hours of incubation the cells were assessed and the spent media was aspirated before dispensing 15 ml of fresh media and returning the flask to the incubator for 3 days.

The period of 3 days allowed the cells to become confluent. The cells were detached from the flask using

5 ml Trypsin-EDTA (Sigma-Aldrich, UK) whilst placed in the incubator for seven minutes. Once all cells had become detached 10ml culture medium was added to neutralize the Trypsin. In order to aspirate the supernatant the cell culture was centrifuged (U-320R; Boeco, GmbH) for five minutes at 200 g. To ensure the cells were ready for seeding they were resuspended in 10 ml of culture medium and dispensed between the eighteen samples in the 6-well plates. This equated to 0.55 ml ( $2 \times 10^4$  cells/ml) for each sample. Plate 2 was removed from incubation after 24 hours and plates 3 and 4 after 4 days. Plates 2 and 3 were prepared for the SEM and plate 4 was prepared for counting using an improved Neubauer hemacytometer (Fisher Scientific, UK).

### SEM Analysis of *In Vitro* Samples

The samples were initially rinsed with phosphate-buffered saline (PBS) (Sigma-Aldrich, UK) to remove any unattached cells and then adherent cells were fixed using 1.2% glutaraldehyde in water (Sigma-Aldrich, UK) at room temperature for 1 hour. After an hour the glutaraldehyde solution was removed and the fixed cells were washed with PBS prior to carrying out a graded series of ethanol/distilled water mixtures of 50/50, 80/20, 90/10, 95/5, 98/2 and 100/0. Each sample was left in these mixtures for 10 minutes. The samples were then mounted and sputter coated with Au so that SEM images could be obtained.

## Results and Discussion

### Effect of Laser Processing on Topography

Through Figures 1 and 2 it can be deduced that the laser patterned samples had considerably rougher

surfaces with the largest peak heights being of the order of 2  $\mu\text{m}$  for the laser patterned samples (see Figure 2) in contrast to the as-received sample (see Figure 1) which had peaks heights of up to 0.2  $\mu\text{m}$ .

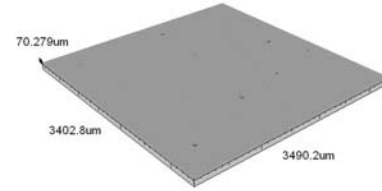


Figure 1 – Continuous axonometric and profile extraction for the as-received sample (AR).

Continuous axonometric images and profile extractions of the whole area irradiated samples can be seen in Figure 3. In comparison to the laser patterned samples (see Figure 2) the whole area irradiated samples, shown in Figure 3, highlight that there was considerable more melting which can be identified firstly through craters left from evolved gases breaking at the surface. This is especially apparent for the whole area irradiated samples which had larger incident fluences (see Figure 3(e) and (f)). Also, the fluence used for samples WA17 (see Figures 3(a) and WA26 (see Figures 3(b)) was close to that of the threshold, allowing for a similar topography exhibited by the as-received sample (see Figure 1).

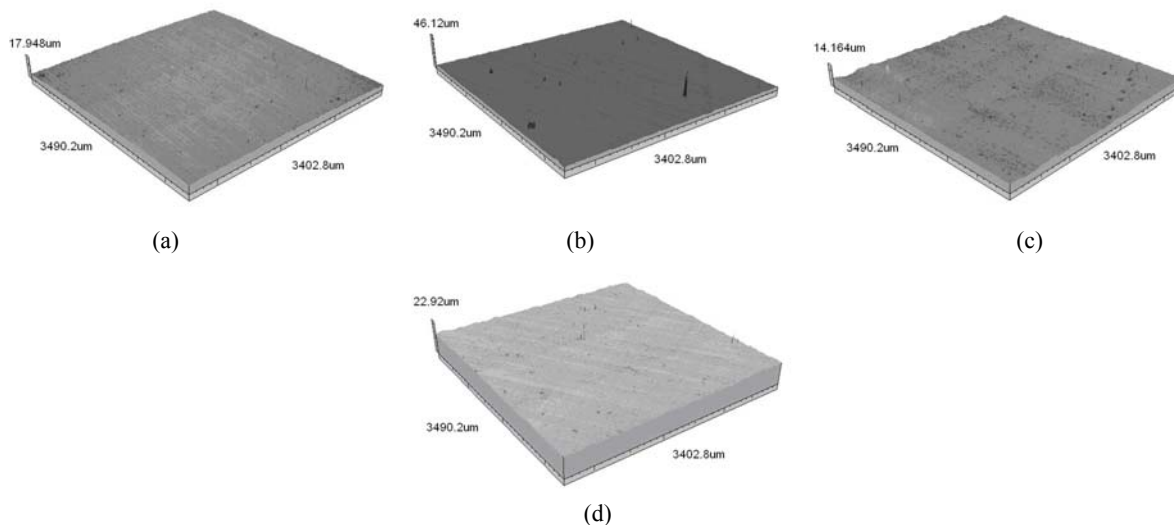


Figure 2 – Continuous axonometric images for (a) T50 (b) T100 (d) H50 and (d) H100.

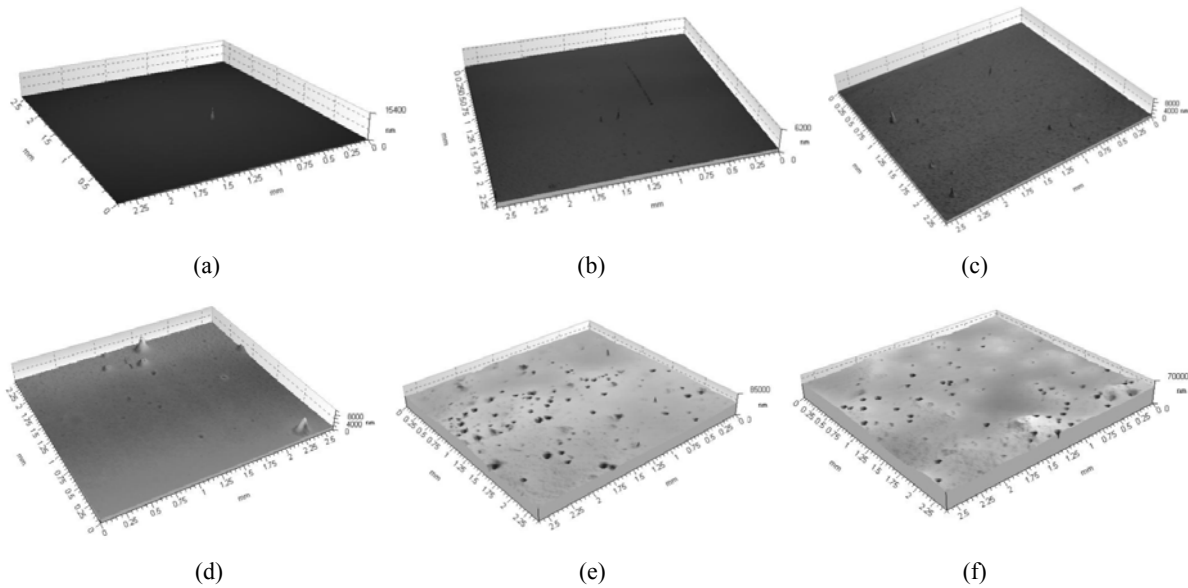


Figure 3 – Continuous axonometric images of samples (a) WA17, (b) WA26, (c) WA34, (d) WA51, (e) WA102 and (f) WA128.

### Effect of Laser Processing on Wettability

Table 1 gives a summary of the results obtained for each of the nylon 6,6 samples. For all samples with the exception of whole area samples WA17 and WA26 there was a significant variation in all parameters such that the surface roughness and surface oxygen content had increased in comparison to the as-received sample (AR). For samples WA17 and WA26, the results obtained for these samples can be seen to be equivalent to that of the as-received sample (AR) owed to the low fluences implemented.

In general, for the laser-patterned samples the surface roughness increased considerably with the largest Sa of 0.4  $\mu\text{m}$  being achieved with the H50 sample and largest Ra of 0.2  $\mu\text{m}$  for the T100 sample. This can be seen to be significant as current theory states that for a hydrophilic material such as nylon 6,6 an increase in roughness should bring about a reduction in the characteristic contact angle [1]. However, in this instance this is not the case as the contact angle had increased for all laser-patterned samples. As hypothesized previously [10,12], this phenomenon can be explained by the likely existence of a mixed-state wetting regime in which both Cassie-Baxter and Wenzel wetting regimes are present across the solid-liquid interface [13-16]. On the other hand, for the whole area irradiated samples, it can be seen that the largest surface roughness arises from samples WA102 and WA128 with Sa of 4 and 3  $\mu\text{m}$ , respectively. These samples appear to correspond with current theory such that the reduction in contact angle arises

from the surface roughness increasing, polar component and total surface energy increasing.

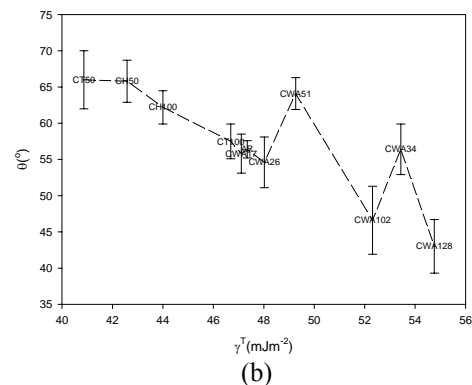
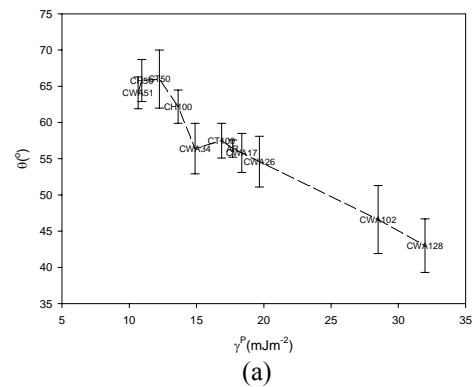


Figure 4 – Graphs showing the correlation between  $\theta$  and (a)  $\gamma^p$  and (b)  $\gamma^T$ .

Table 1 – Results summary for all samples showing roughness parameters, surface oxygen content and wettability characteristics.

Sample ID	Sa ( $\mu\text{m}$ )	Ra ( $\mu\text{m}$ )	$\gamma^p$ ( $\text{mJm}^{-2}$ )	$\gamma^D$ ( $\text{mJm}^{-2}$ )	$\gamma^T$ ( $\text{mJm}^{-2}$ )	Surface Oxygen Content (%at.)	Contact Angle ( $^\circ$ )
AR	0.126	0.029	17.69	29.66	47.34	13.26	56.4 $\pm$ 1.2
CT50	0.636	0.148	12.24	28.63	40.87	14.33	66.0 $\pm$ 4.0
CT100	0.297	0.185	16.86	29.83	46.69	14.05	57.5 $\pm$ 2.4
CH50	0.423	0.103	10.93	31.64	42.58	14.99	65.8 $\pm$ 2.9
CH100	0.326	0.155	13.63	30.37	44.00	14.84	62.2 $\pm$ 2.3
CWA17	0.111	0.060	18.36	28.75	47.11	13.56	55.8 $\pm$ 2.7
CWA26	0.100	0.158	19.67	28.35	48.02	13.86	54.6 $\pm$ 3.5
CWA34	0.101	0.092	14.89	38.55	53.43	14.34	56.4 $\pm$ 3.5
CWA51	0.341	0.139	10.66	38.59	49.26	15.45	64.1 $\pm$ 2.2
CWA102	4.356	1.236	28.49	23.82	52.31	16.77	46.6 $\pm$ 4.7
CWA128	3.201	1.335	31.98	22.78	54.76	18.93	43.0 $\pm$ 3.7

Figure 4 allows one to see that  $\theta$  was a decreasing function of  $\gamma^p$  and  $\gamma^T$  indicating that the surface energy played a major role in the determination of the wettability characteristics of nylon 6,6.

#### Effect of Laser Processing on Osteoblast Cell Response: 24 Hours

It can be seen in Figures 5, 6 and 7 that for all samples the osteoblast cells have to some extent adhered to the differing surfaces. That is, the cells have firstly attached, adhered and have begun to spread across the surfaces. The extent to which this phenomenon has taken place appears to be dependent on the laser processing owed to the larger areas of cell coverage after 24 hours of incubation time. From the micrographs shown in Figures 5, 6 and 7 the laser treated samples do not appear to give rise to directionality in terms of cell growth. In terms of cell morphology the micrographs in Figures 5, 6 and 7 show that most of the samples gave rise to bipolar

shapes, apart from the T100 sample (see Figure 7(b)) which was at a more advanced stage of cell growth.

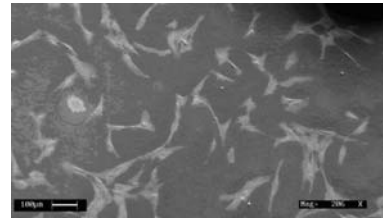


Figure 5 – SEM image of Au coated samples 24 hours post seeding for the as-received sample (AR).

In respect of proliferation, samples WA102 and WA128 gave rise to less proliferation. Furthermore, the cells appeared to be more concentrated in and around the craters and cracks arising from the processing. This may be owed to the possibility of more surface oxygen content being present in these areas giving rise to better cell adhesion.

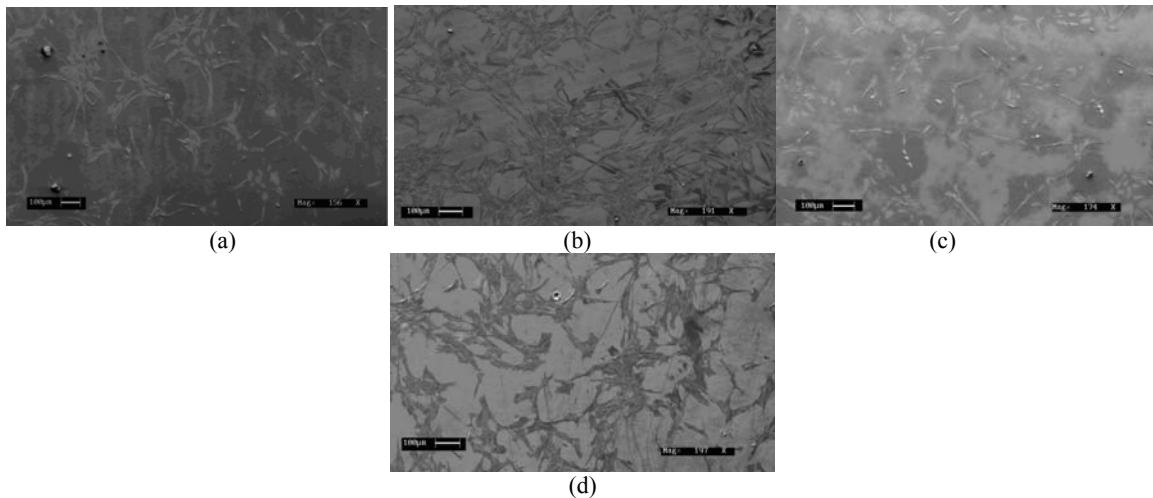


Figure 6 – SEM images of Au coated samples 24 hours post seeding for laser-patterned samples (a) T50 (b) T100 (c) H50 and (d) H100.

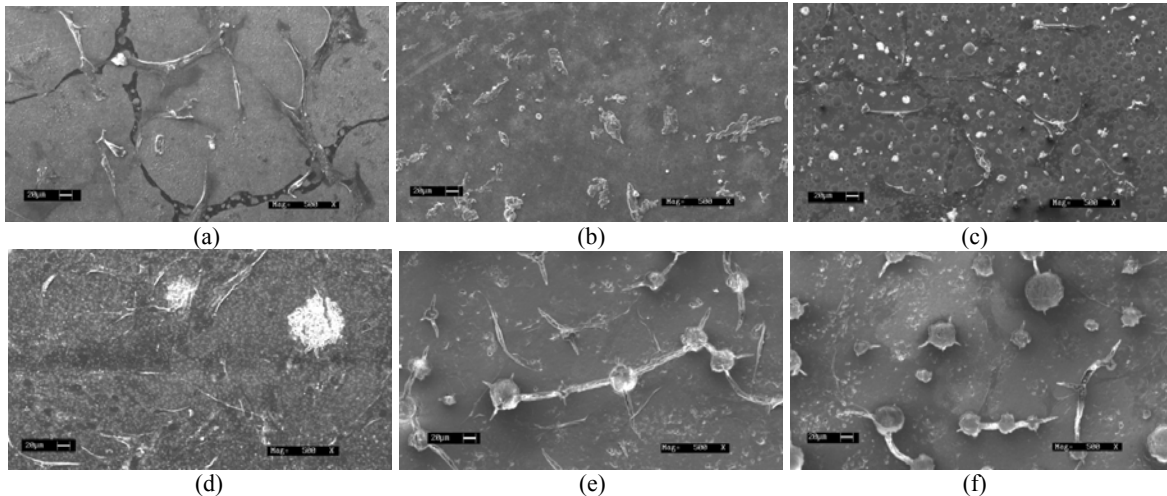


Figure 7 – SEM images of Au coated samples 24 hours post seeding for whole area irradiated samples (a) WA17 (b) WA26 (c) WA34 (d) WA51, (e) WA102 and (d) WA128.

The histogram given in Figure 8 shows that the cover density after 24 hours was larger for most laser irradiated samples in comparison with the as-received sample (AR). Samples WA17 and WA26 gave rise to wettability characteristics similar to the as-received sample (AR) and as a result of this, had a negligible effect on cell response. The largest mean cover density of 38% was achieved with the T100 sample, whilst 17% was observed for the as-received (AR) sample. Samples WA102 and WA128 samples gave the lowest cover densities of 6 and 9%, and can be owed to the samples becoming too toxic.

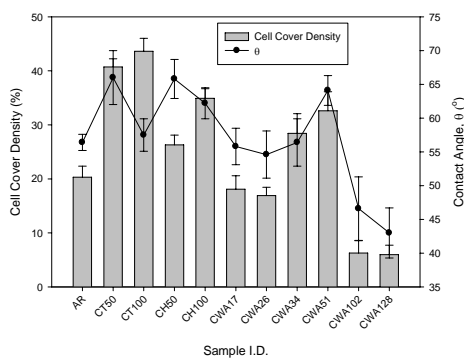


Figure 8 – Histogram showing the cover densities for each of the seeded CO<sub>2</sub> laser processed nylon 6,6 samples after 24 hrs with relation to  $\theta$ .

Figure 8 also shows the possible relationship between the cell cover density and  $\theta$ . For the whole area irradiative processed samples it was found that there was a somewhat linear relationship between the cell cover density and  $\theta$ . In contrast, Figure 8 highlights

that there was no correlative relationship between the cell cover density and  $\theta$  for the laser-induced patterned samples. This can be attributed to the mixed-state wetting regime leading to erroneous results.

#### Effect of Laser Processing on Osteoblast Cell Response: 4 Days

From Figures 9, 10 and 11 it is evident that the cells had rapidly begun to proliferate over the 4 day incubation period such that for most samples the cover density was tending towards maximum 100%.



Figure 9 – SEM micrograph after 4 days incubation for sample AR.

In terms of cell morphology, it was established that the as-received (AR) sample (see Figure 9) gave rise to a more coral-like morphology. The 50  $\mu$ m trench (T50) patterned sample (see Figure 10(a)) gave a cell morphology which was more clumped, spindle-like, growing in a radial nature. The 100  $\mu$ m trench patterned (T100) sample (see Figure 10(b)) was seen to produce a clumped radial cell morphology. Whereas the two hatch patterns (H50 and H100) (see Figures 10(c) and (d)) had cell morphologies which were clumped radial with the 50  $\mu$ m trench pattern (see Figure 10(c)) appearing to be more coral-like.

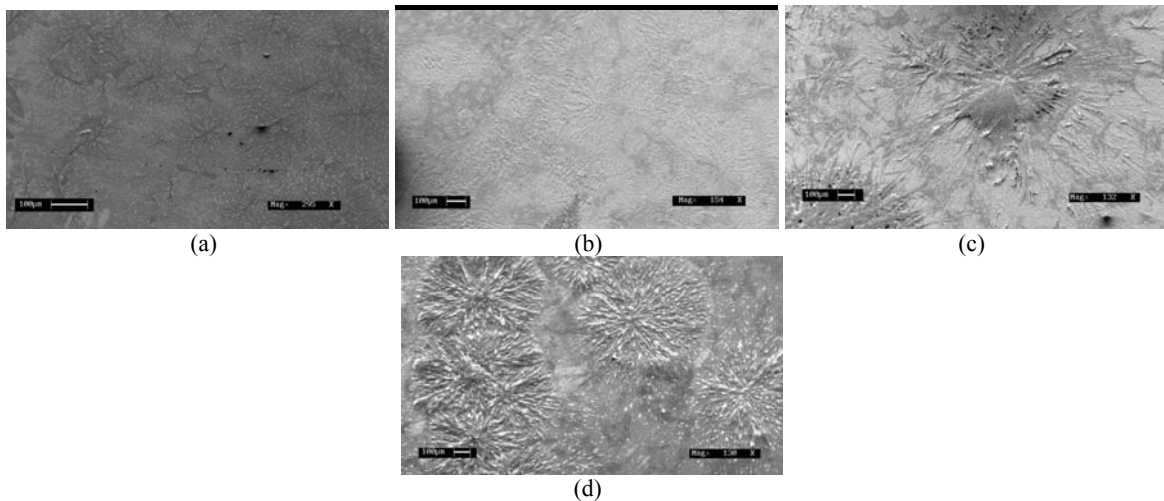


Figure 10 – SEM images of Au coated samples after 4 days incubation for laser-patterned samples (a) T50 (b) T100 (c) H50 and (d) H100.

For the whole area irradiated samples (see Figure 11) the morphologies were somewhat different. WA17 (see Figure 11(a)) gave rise to a clumped morphology which was slightly spindle-like. Whereas samples WA26, WA34 and WA51 (see Figures 11(b), (c) and (d) respectively) gave rise to spindle-like morphologies with larger filopodia as the incident fluence increased. Finally, samples WA102 and WA128 (see Figures 11(e) and (f), respectively) gave rise to morphologies that were similar to that observed after 24 hours in that the cells were bipolar in nature.

On average, for each sample the cover density was approximately tending towards 100% apart from WA102 and WA128. Sample WA102 and sample WA128 gave rise to cover densities of 76 and 58%, respectively and as a result there could be some

correlation between how the nylon 6,6 was treated and how the osteoblast cells reacted to the samples *in vitro*. The reasoning for the reduced cover densities for samples WA102 and WA128 in comparison to the other samples is that these samples are likely to have become more toxic which would ultimately hinder osteoblast cell growth [17].

A graph of cell count can be seen in Figure 12 which indicates that there was a higher cell count after 4 days incubation for all samples apart from samples WA102 and WA128. Even though WA102 and WA128 did not promote enhanced cell adhesion and proliferation, the other results obtained indicate that the laser surface treatment had a significant effect on the cell response in terms of cell cover density and growth.

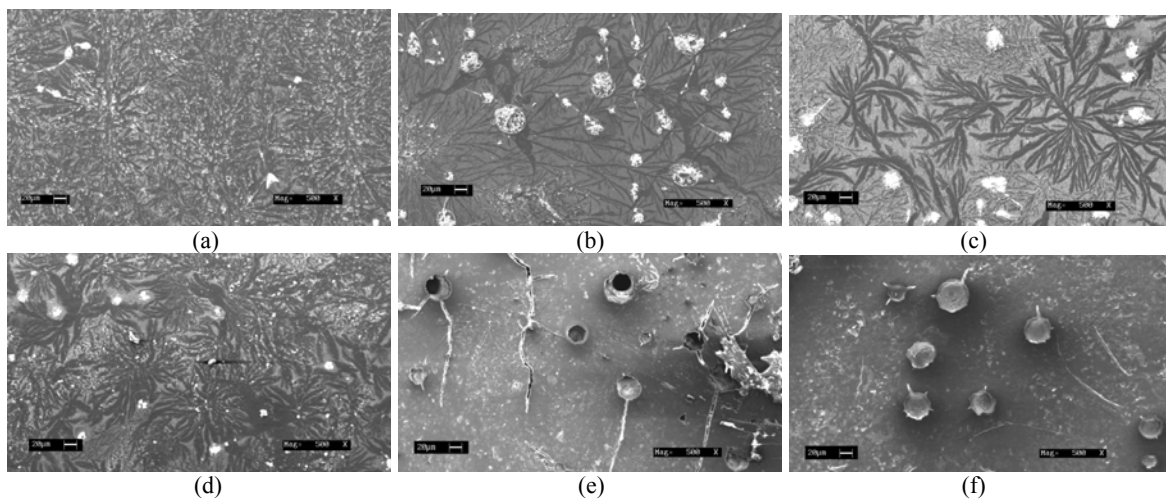


Figure 11 – SEM images of Au coated samples after 4 days incubation for whole area irradiated samples (a) WA17 (b) WA26 (c) WA34 (d) WA51, (e) WA102 and (f) WA128.

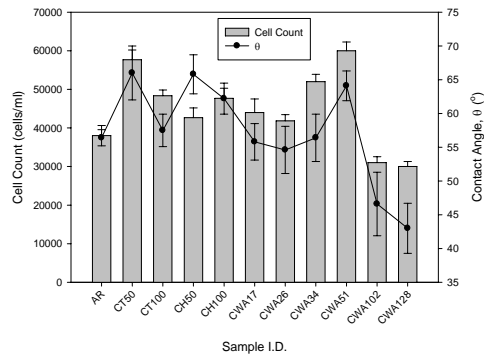


Figure 12 – Histogram showing the cell count for each of the seeded CO<sub>2</sub> laser processed nylon 6,6 samples after 24 hrs in relation to  $\theta$ .

Similar to what was observed with the cell cover density (see Figure 8), the whole area irradiative processed samples gave rise to a linear response between the cell count and  $\theta$ . Whereas, the laser-induced patterned samples giving rise to a mixed-state wetting regime did not tend to follow any particular trend. What is more, on account of the strong relationship between  $\theta$  and  $\gamma^p$  (see Figure 4), for the laser whole area irradiative processed samples the osteoblast cell response in terms of  $\gamma^p$  was found to be the inverse of what was determined for  $\theta$ .

With the laser-induced patterning giving rise to erroneous results when considering trends between the osteoblast cell response and laser-induced wettability characteristic modifications, it is possible to deduce that predicting the biomimetic nature of these samples would prove to be very difficult. However, it has been established that for the whole area irradiative processing the osteoblast cell response does follow some correlative trend with both  $\theta$  and  $\gamma^p$ . As a result of this it is possible to ascertain that this makes inroads to the potential use of laser surface treated nylon 6,6 within regenerative medicine on account of the results being shown to be predictable.

### Generic Wettability Characteristics that Determine the Biomimetic Nature of Nylon 6,6

It has previously been determined that  $\theta$  was a decreasing function of both  $\gamma^p$  (see Figure 4(a)) and  $\gamma^T$  (see Figure 4(b)). In addition to this, Figure 8 and Figure 12 elude to a possible relationship between the wettability characteristics and the osteoblast cell response elicited by the laser surface treated nylon 6,6

samples, especially for those samples which had undergone laser whole area irradiative processing.

Figure 13 shows that there was a strong relationship between the cell cover density and the wetting nature of the nylon 6,6 for the laser whole area irradiative processed samples. That is, the cell cover density was an increasing function of  $\theta$ . In a similar manner, owed to the strong relationship between  $\theta$  and  $\gamma^p$  (see Figure 4(a)), the cell cover density was found to be a decreasing function of  $\gamma^p$ . With the inverse relationship observed this serves to give further evidence of the strong link between  $\theta$  and  $\gamma^p$ . Having said that, a number of data points shown in Figure 13 allow one to see that the laser-induced patterned samples did not appear to fit any particular trend. This could be on account of the fact that a transition in wetting regime was likely to have played a significant role in the biomimetic nature of the nylon 6,6.

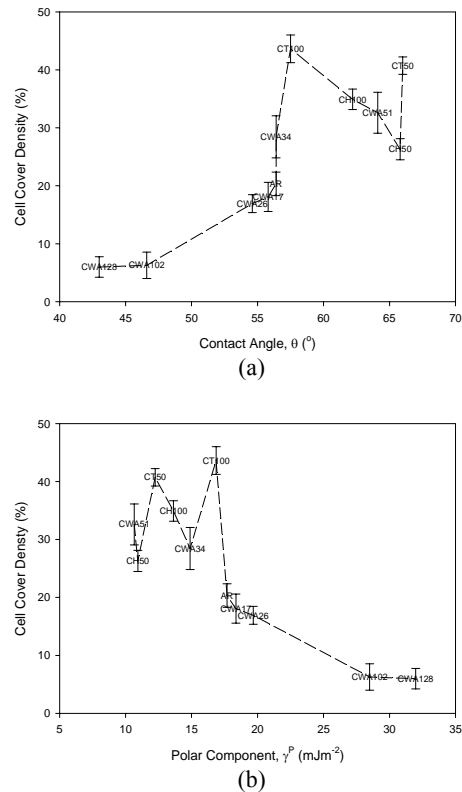


Figure 13 – Graphs showing the relationship between (a)  $\theta$ , (b)  $\gamma^p$  and cell cover density.

With respect of the cell count following four days incubation, it can be seen from Figure 14 that the cell count followed similar correlative trends as to what

was determined for the cell cover density (see Figure 13). Since, the cell count was found to be an increasing function of  $\theta$  (see Figure 14(a)) and a decreasing function of  $\gamma^p$ , especially for those samples which did not give rise to a likely transition in wetting regime.

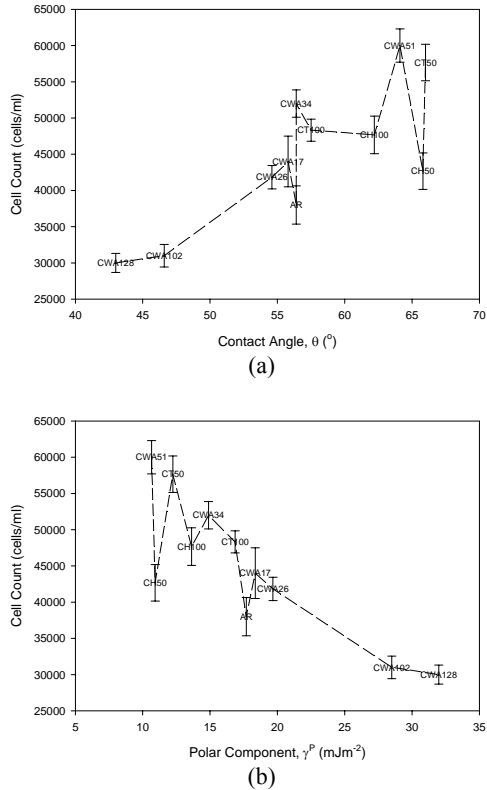


Figure 14 – Graphs showing the relationship between (a)  $\theta$ , (b)  $\gamma^p$  and cell count.

In terms of the other surface parameters it was found that no other factor studied, such as  $\gamma^T$  or surface oxygen content did not appear to play a significant role in the biomimetic nature of laser surface treated nylon 6,6. As a result of this, one can reasonably say that  $\theta$  and  $\gamma^p$  played a dominant part in the determination of the bioactive nature in terms of osteoblast cell response. What is more, this opens an attractive means of predicting the biomimetic properties of nylon 6,6 which has the potential to be applied to other polymeric materials.

## Conclusions

Through this study it has been demonstrated that following CO<sub>2</sub> laser processing of nylon 6,6 the surface characteristics can be modified in order to have influence over the contact angle. From analysing the laser induced patterned surfaces it was found that the surface energy and polar component had decreased by

up to 7 mJm<sup>-2</sup> and the surface roughness had considerably increased. It was found that the contact angle was a decreasing function of the polar component and total surface energy, which correlates with current theory. Current theory states that the contact angle for a hydrophilic surface should decrease upon increasing surface roughness which has not been seen throughout this experimentation. This was observed for the CO<sub>2</sub> laser whole area irradiative processed samples and not for the CO<sub>2</sub> laser-induced patterned samples. This phenomena can be attributed to an intermediate mixed Cassie-Baxter/Wenzel regime, in which both Wenzel and Cassie-Baxter regimes arise at the solid-liquid interface. From the results obtained it was found that the apparent surface energy and its components were the most dominating parameter in the modification of wettability which was a result of the mixed state wetting regime owed to the surface topography produced from the different laser-induced patterns.

It has been seen that for most of the CO<sub>2</sub> laser surface treated nylon 6,6 samples, osteoblast cell response has been improved to become more efficient, allowing cell growth to become quicker. This has been seen through the fact that the cells have covered more area of the nylon 6,6 samples after 24 hours and that the cell density count had increased after 4 days in comparison with the as-received (AR) sample. However, samples WA102 and WA128 did not appear to promote an enhanced biomimetic surface resulting in the surfaces hindering cell adhesion and proliferation. This is likely to be due to an increase in surface toxicity. Nevertheless, the results obtained imply that, below a certain threshold, the laser surface treated nylon 6,6 gave rise to enhanced biomimetic properties for nylon 6,6. Significantly, it has been seen that over 24 hours and 4 day incubation periods samples WA34, WA51, T50 and T100 gave rise to improved cell response, having greater cell cover density and mean cell count density in comparison with both the other laser surface treated samples and as-received reference control samples.

Ultimately, it has been established that the contact angle had a strong correlation with the surface energy and induced-patterned. In addition to this, for the laser whole area irradiative processed nylon 6,6 samples the wettability of nylon 6,6 had a strong link between the bioactive nature of the samples. This leads to one realizing the large potential laser surface treatment has for applications within regenerative medicine.

## Acknowledgements

The authors would like to thank their collaborators: Directed Light Inc., East Midlands NHS Innovation

Hub, Nobel Biocare and Photomachining Inc. for all of their much appreciated support. The authors greatly acknowledge the Access to Research Equipment Initiative funded by the EPSRC (EP/F019823/1) and would like to thank Chemical Engineering, Loughborough University for use of their biological laboratory. This study is also financially supported by the EPSRC (EP/E046851/1).

## References

1. Hao, L. & Lawrence, J. (2005) Laser surface treatment of bio-implant materials. New Jersey, USA: John Wiley & Sons Inc.
2. Wirth, C., Grosogeat, B. & Lagneu, C. *et al* (2008) Biomaterial surface properties modulate *in vitro* rat calvaria osteoblasts response: Roughness and or chemistry? *Materials Science and Engineering C*, 28 990.-1001
3. Lim, J.Y., Hansen, J.C. & Siedlecki, C.A. *et al.* (2005) Human foetal osteoblastic cell response to polymer-demixed nanopopographic interfaces. *Journal of the Royal Society Interface* 2 97-108.
4. Hao, L., Lawrence, J. & Lin, L. (2005) Manipulation of the osteoblast response to a Ti-6Al-4V titanium alloy using a high power diode laser. *Applied Surface Science* 247 602-606.
5. Paital, S.R. & Dahotre, N.B. (2009) Calcium phosphate coatings for bio-implant applications: Materials, performance factors and methodologies. *Materials Science and Engineering R* 66 1-70.
6. Vogler E.A. (1993) *Interfacial chemistry in biomaterials science*. New York, USA: Marcel Dekker.
7. Arefi-Khonsari, F., Tatoulian, M. & Bretagnol, F. *et al* (2005) Processing of polymers by plasma technologies. *Surface and Coatings Technology* 200 14-20.
8. Dadbin, S. (2002) Surface modification of LDPE film by CO<sub>2</sub> pulsed laser irradiation. *European Polymer Journal* 38 2489-2495.
9. Wochnowski, C., Hanada, Y. & Cheng, Y. *et al* (2006) Femtosecond-laser-assisted wet chemical etching of polymer materials. *Journal of Applied Polymer Science* 100 1229-1238.
10. Waugh, D.G., Lawrence, J. & Morgan, D.J. (2009) Interaction of CO<sub>2</sub> laser-modified nylon with osteoblast cells in relation to wettability. *Materials Science in Engineering C* 29 2514-2524.
11. Rance, D.G. (1982) Chapter 6 - thermodynamics of wetting: From its molecular basis to technological application. In: Brewis, D.M. (ed.) *Surface Analysis and Pretreatment of Plastics and Metals*. Essex, UK: Applied Science Publishers, pp.121.
12. Waugh, D.G., Lawrence, J. & Walton C.D. (2010) On the effects of using CO<sub>2</sub> and F<sub>2</sub> lasers to modify the wettability of a polymeric biomaterial. *Journal of Optics and Laser Technology* 42 347-356.
13. Lee, S.M. & Kwon, T.H. (2007) Effects of intrinsic hydrophobicity on wettability of polymer replicas of a superhydrophobic lotus leaf. *Journal of Micromechanics and Microengineering* 17 687-692.
14. Cheng, Y.T. & Rodak, D.E. (2005) Is the lotus leaf superhydrophobic? *Applied Physics Letters* 86 144101/1-144101/3.
15. Chen, X. & Lu, T. (2009) The apparent state of droplets on a rough surface. *Science in China Series G* 52 233-238.
16. Wu, X., Zheng, L. & Wu D. (2005) Fabrication of superhydrophobic surfaces from microstructured ZnO-based surfaces via a wet-chemical route. *Langmuir* 21 2665-2667.
17. Cook, S.D., Ryaby, J.P. & McCabe, J.R.N. *et al* (1997) Acceleration of tibia and distal radius fracture healing in patients who smoke. *Clinical Orthopaedics and Related Research* 337 198-207.
18. Nebe, B., Luthen, F. & Lange, R. *et al.* (2004) Topography-induced alterations in adhesion structures affect mineralization in human osteoblasts on titanium. *Materials Science in Engineering C* 24 619-624.

## Meet The Author

David Waugh is currently undertaking a Ph.D. at the Wolfson School of Mechanical and Manufacturing Engineering, Loughborough University, UK under the supervision of Dr. Jonathan Lawrence. His research is focusing on using laser surface treatment of polymeric biomaterials for enhanced cell response. He obtained his MPhys Hons. in Physics with Lasers and Photonics and MSc in Laser Applications in Micro-Machining and Processing from the University of Hull, UK.